Enhanced aluminum alloy-polymer friction stir welding joints by introducing micro-textures

Wenquan Wang[a], Suyu Wang[a], Xinge Zhang[a, *], Yuxin Xu[a], Yingtao Tian[b], Hu Huang[c]

[a]Key Laboratory of Automobile Materials of Ministry of Education, School of Materials Science and Engineering, Jilin University, No. 5988 Renmin Street, Changchun, 130025, China

[b]Department of Engineering, Lancaster University, Bailring, Lancaster LA1 4YW, United Kingdom

[c]School of Mechanical and Aerospace Engineering, Jilin University, Changchun, Jilin, 130025, China

* Corresponding author.

E-mail address: zhangxinge@jlu.edu.cn

Abstract

In this work, a micro-texture through laser ablation pre-treatment on aluminum alloy surface was designed, which successfully induced high bonding strength of aluminum alloy-polymer friction stir welding joints. The bonding mechanism of aluminum alloy-polymer was attributed to the large mechanical interlocking from the geometric grooves in micro-textures and the formation of C-O-Al bond at the interfaces. This study provides new insight of friction stir welding of metal and polymer through controllable surface pre-treatments.

Keywords: Metals and alloys; Polymers; Laser processing; Welding.

1. Introduction

The development of a wide range of lightweight materials and corresponding joining techniques are driven by the compelling need for energy-efficient and environment-friendly engineering [1]. Known for the advantages of high specific strength and low density, aluminum (Al) alloy and polymer have become potential candidates for automobile and aerospace devices [2]. Thus, the reliable joining of Al alloy and polymer has been considered as a key issue for lightweight design and manufacturing.

Importantly, laser welding processes were considered to develop reliable joining of metals and polymers [3], but the high volume of bubbles at bonding interfaces were regarded as major defects, which limited practical engineering applications [4]. As a solid-state welding technique, friction stir welding (FSW) shows huge advantages to join Al alloy and polymer due to lower heat input and real time tracking pressure [5]. F Yusof et al. utilized friction spot welding process to join Al alloy and PET, and the maximum tensile load of 900N was obtained [6]. Furthermore, for the purpose of increasing the mechanical interlocking of Al alloy-polymer joints, numerous works were conducted on the novel design of welding tool. For instance, Yongxian huang et al. designed a taper-screwed pin with triple facets which could enhance material flow and improve mechanical performance of metal-polymer joints efficiently [7]. Nevertheless, these methods draw on the characteristics of mechanical fastening and undermined the integrity of base materials. Additionally, F.C. Liu presented a friction lap welding technique for direct joining of polymer to Al alloy, and the joints with superior integrity but lower mechanical interlocking were produced [8]. With the aim of increasing joint strength, functionalization of base material surfaces is of vital importance, and laser ablation process could introduce micro-patterning structure on Al alloy surface to enhance interfacial bonding effectively [9]. However, few studies are explored on the enhanced metal-polymer FSW joints through laser ablation pre-treatment, so as the underlying bonding mechanism.

Accordingly, in this work, a rotation tool with an ultra-short rotational pin was designed to ensure the joint integrity. In addition, laser ablation process was conducted on Al alloy surface, and FSW process was proposed to join Al alloy and polymer. Ablation micro-morphology, interface characterization and bonding mechanism were investigated in detail.

2. Experimental procedures

The polyamide 6 (PA6) and 6061 aluminum alloy sheets with the thickness of 1.5 mm were used as base materials. The dimensions of specimens and welding tool are shown in Fig. 1(a). The micro-textures on A6061 surface were built by a fiber nanosecond pulsed laser (SP-050P-A-EP-Z-F-Y, SPI Lasers, UK). The confocal scanning microscope LEXT OLS3000 was used to observe the 3D view of the micro-textures. Micro-morphology of the grooves and the interfaces of joints were observed by scanning electron microscopy (SEM, TESCANVEGA3). The interfacial chemical bonds were characterized by X-ray photoelectron spectroscopy (XPS, ESCALAB 250 spectrometer). Shear-tensile tests of joints were conducted on the electro-hydraulic servo testing machine (MST 810) with the constant speed of 1 mm/min, and each data point of tensile-shear tests was the average value of five specimens under the same conditions.

3. Results and discussion

The design of ultra-short stir pin can not only improve the stability of rotational welding tool to ensure the superior formability of joints, as shown in Fig. 1(b), but also provide bending force to enhance the joint performance. As revealed in Fig. 1(c), under the thermal-mechanical behavior of FSW process, the embedded PA6 in the grooves provided strong mechanical interlocking. Fig. 1(d) shows 3D view of micro-patterning structure produced on A6061, it can be clearly seen that the processed grooves had certain regularity and controllability. Moreover, the geometric features of grooves can be easily adjusted by varying the parameters of laser ablation, which was able to affect the joint performance significantly.

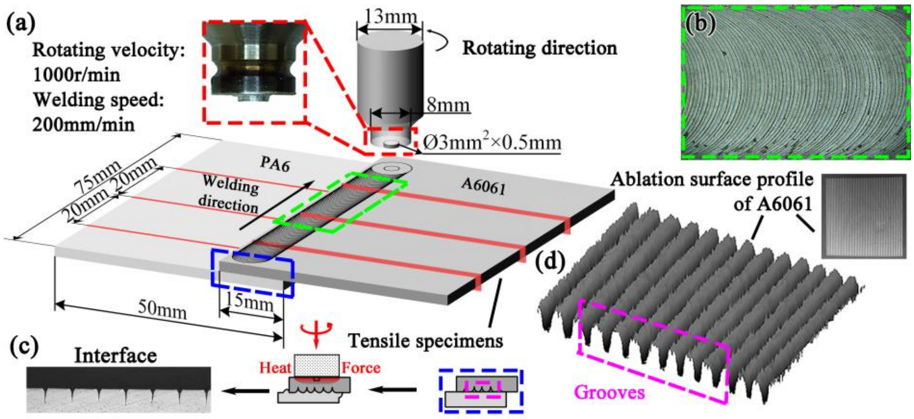

Fig.1 Schematic of the FSW process: (a) illustration of welding tool and specimen dimensions; (b) the top view of weld; (c) illustration of thermal-mechanical behavior in FSW; (d) 3D view of micro-textures produced on A6061.

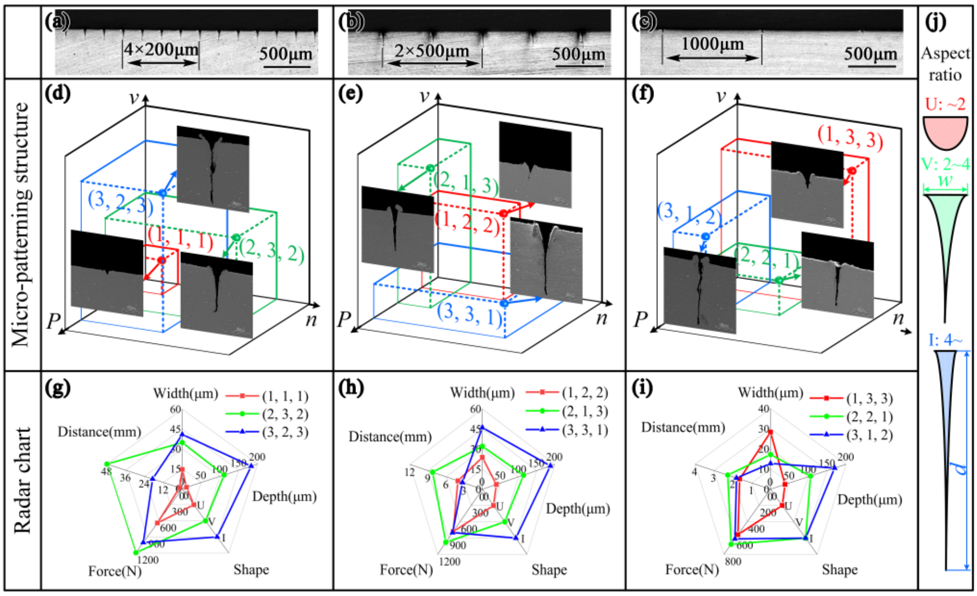

Fig.2 (a)-(c) Spacing between grooves under different laser ablation parameters; (d)-(f) micro-morphology of grooves showing the variation in geometry; (g)-(i) radar chart of the geometric features versus mechanical properties; (j) illustration of typical morphology of grooves.

The laser power (10 W, 15 W, 20 W), scanning times (1, 5, 10), scanning speed (10 mm/s, 15 mm/s, 20 mm/s) and scanning spacing (200 μm, 500 μm, 1000 μm) were chosen as variables of the laser ablation process, and a $L_9(3^4)$ orthogonal test was carried out in this work. As shown in Fig.2, the laser power P, scanning times *n*, scanning speed *v* which could affect the geometry of the grooves directly were set as *x*, *y*, *z* axes, and scanning spacing *h* was set as the external axis to construct an orthogonal space. Furthermore, the three levels of each factor were marked as "1, 2, 3" from low to high, for instance, (1, 1, 1) represented laser power of 10 W, scanning times of 1 and scanning speed of 10 mm/s. Each point in the space represented a group of parameters, and 9 independent groups out of whole 81 (3^4) groups were chosen in the orthogonal experiment, as reflected in Fig. 2(d)-(f). Furthermore, the morphology of grooves was mainly divided into three types (U-shaped, V-shaped and I-shaped), which were determined by aspect ratio (groove depth *d* / groove width *w*) [10], as shown in Fig.2 (j). In order to verify whether the groove geometry has an effect on joint performance, radar charts of the geometric features versus mechanical properties were established. The U-shaped grooves can be identified with small aspect ratio (<2), and it is easy to be completely peeled off during the tensile test due to a small contact area between grooves and embedded PA6. The I-shaped grooves can be identified with large aspect ratio (>4), so the grooves were easily closed due to the cold shrinkage of metals, which caused the poor performance of joints. The balanced shear and tensile capabilities of embedded PA6 was obtained owing to the moderate aspect ratio (2~4) of V-shaped grooves, indicating enhanced bonding of A6061-PA6 joints. In addition, the groove density was determined by scanning spacing and the joint strength increased notably with larger groove density. Enhanced interfacial bonding can be achieved with the scanning space of 200 μm, but increasing groove density with prolonging consuming time does not yield a further significant increase of joint strength.

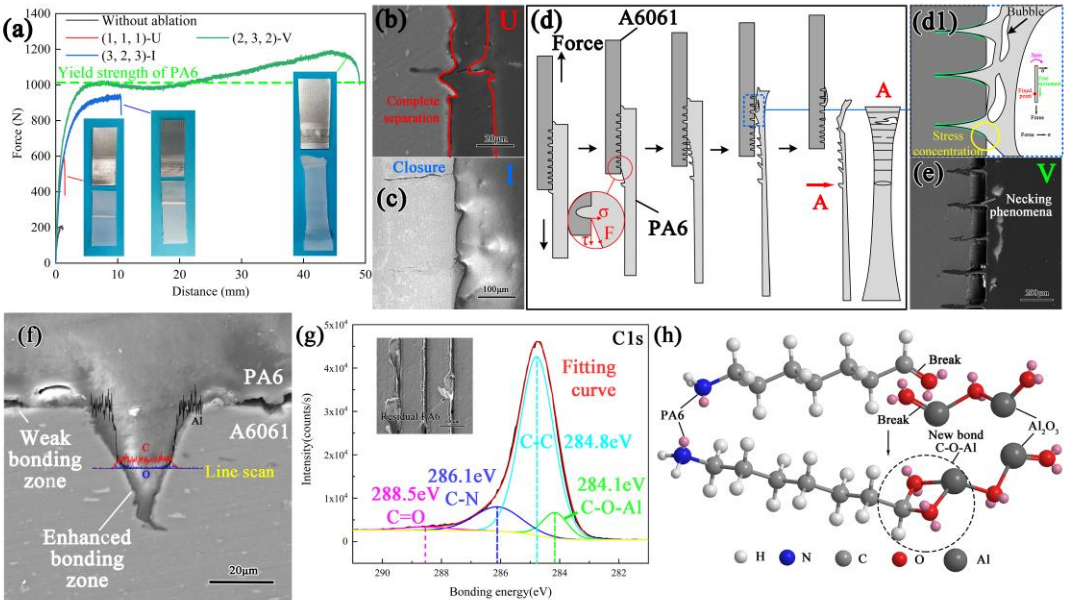

Fig.3 (a) Force-distance curve of A6061-PA6 joints; (b) complete separation of U-shaped grooves; (c)closure phenomenon of I-shaped grooves; (d)illustration of fracture mechanism; (e) semi-extracted state of V-shaped grooves;(f) morphology of the groove interface and line scan results; (g) XPS analysis of fracture surface on A6061 side; (h) schematic illustrations of C-O-Al bond formation.

In order to further investigate the effects of groove geometry on bonding and fracture mechanism of joints, the tensile curves of (1, 1, 1) specimen (U-shaped grooves), (2, 3, 2) specimen (V-shaped grooves), (3, 2, 3) specimen (I-shaped grooves) and specimen without laser ablation pre-treatment are exhibited in Fig. 3(a). For joints obtained with V-shaped grooves, the PA6 substrate underwent severe plastic deformation and then broke on the PA6 substrate with the maximum shear-tensile load of 1194 N which has reached the yield strength of PA6 base material (the cross-sectional dimension of PA6 was 20 mm × 1.5 mm), indicating the feasibility of the surface pre-treatments to promote the performance of metal-polymer joints. In addition, U-shaped grooves with poor tensile load resistance showed complete separation, while I-shaped grooves with tiny width led to the reduce of embedded PA6 and even the occurrence of closure phenomenon, which degraded the mechanical interlocking effect, as shown in Fig.

3(b)-(c). Fig. 3(d)-(e) shows the fracture mechanism of joints with V-shaped grooves, it can be seen that PA6 gradually elongated with the decrease of thickness, and the stress state of forefront grooves was reflected in the red circle. Notably, it can be seen that the embedded PA6 could not be pulled out by normal stress σ (Fig. 3d1), resulting in a semi-extracted state with necking phenomenon, which proved that a relatively strong bonding was achieved in the grooves. As reflected in Fig. 3(f), the edge of grooves was identified with enhanced bonding zone, while the untreated smooth surface was considered as weak bonding zone which induced the crack initiation and propagation. Additionally, the line scan analysis of the groove interface revealed a transition layer with the thickness of 3.6μm, indicating the occurrence of element diffusion between A6061 and PA6. Furthermore, residual PA6 can also be found on fracture surface in Fig. 3(g), which was contrary to what some scholars have claimed that mainly mechanical interlocking existed between Al alloy and polymer [11]. In order to explore the existence of chemical bonding, XPS analysis was performed on the fracture surface of A6061. In addition to the C-C, C-N (14.25 at. %) and C=O (2.09 at. %) bonds contained in PA6 substrate, the C-O-Al (8.08 at. %) peaks were also found from the XPS results, proving that covalent bonds can be formed between the PA6 and A6061. P. Hirchenhahn et al. also discovered the existence of this bond, and believed that the formation of C-O-Al bond was most likely related to carbonyl group in PA6 molecule and Al_2O_3 on Al alloy surface [12]. In this work, the content of C-O-Al bond was similar to that of C-N bond, so it can be proposed that the single-section PA6 molecule may produce more than one C-O-Al bond. Moreover, owing to the coupling effect of uneven oxide film on the surface of processed grooves and the thermal–mechanical behavior during the FSW process, the C=O bond and Al=O bond broke and recombined to form a long chain structure, as reflected in Fig. 3 (h).

Conclusion

The robust A6061-PA6 FSW joints were obtained successfully through laser ablation pre-treatment on A6061 surface. The processed grooves with certain regularity and controllability improved the mechanical interlocking of joints significantly. Additionally, the coupling effect of oxide film on the surface of A6061 grooves and the thermal–mechanical behavior during the FSW process promoted the formation of C-O-Al bond, and the fracture occurred at PA6 substrates, indicating enhanced interfacial bonding.

Declaration of Competing Interest

We declare that we have no known competing financial interests or personal relationships that could have appeared to influence the work reported in this paper.

CRediT authorship contribution statement

Wenquan Wang: Writing - review & editing, Funding acquisition. Suyu Wang: Methodology, Writing original draft. Xinge Zhang: Formal analysis, Writing - review & editing. Yuxin Xu: Writing - review & editing. Yingtao Tian: Visualization. Hu Huang: Formal analysis.

Acknowledgments

The authors would like to specifically thank Fundamental Research Funds for the Central Universities, JLU (45120031B004) and Jilin Province Science and Technology Development Plan Project (20200401034GX).

References

[1] J. Moon, H.Y. Ha, K.W. Kim, et al., Sci. Rep., 10(1) (2020) 12140.

[2] A. Kubit, D. Wydrzynski, T. Trzepiecinski, Compos. Struct., 201 (2018) 389-397.

[3] S. Arai, Y. Kawahito, S. Katayama, Mater. Des., 59 (2014) 448-453.

[4] J. Jiao, Q. Zou, Y. Ye, Z. Xu, L. Sheng, Compos. B. Eng., 213 (2021) 108738.

[5] T. Wang, L. Li, M.R. Pallaka, H. Das, S. Whalen, A. Soulami, P. Upadhyay, K.S. Kappagantula, Mater. Des., 198 (2021) 109305.

[6] F. Yusof, Y. Miyashita, N. Seo, Y. Mutoh, R. Sci. Technol. Weld. Joi., 17(7) (2013) 544-549.

[7] Y. Huang, X. Meng, Y. Xie, J. Li, X. Si, Q. Fan, J. Mater. Process. Tec., 268 (2019) 80-86.

[8] F.C. Liu, P. Dong, W. Lu, K. Sun, Appl. Surf. Sci., 466 (2019) 202-209.

[9] J. Jiao, S. Jia, Z. Xu, Y. Ye, L. Sheng, W. Zhang, Compos. B. Eng., 173 (2019) 106911.

[10] E. Rodríguez-Vidal, C. Sanz, J. Lambarri, I. Quintana, Opt. Laser Technol., 104 (2018) 73-82.

[11] S. Zhao, F. Kimura, S. Kadoya, Y. Kajihara, Precis. Eng., 61 (2020) 120-125.

[12] P. Hirchenhahn, A. Al Sayyad, J. Bardon, A. Felten, P. Plapper, L. Houssiau, ACS Appl. Polym. Mater., 2(7) (2020) 2517-2527.